**Mondher Abidi[1,2,*], Amine Ben Rhouma[2,3], Jamel Belhadj[1,2]**

J. Electrical Systems 16-2 (2020): 185-200

**Regular paper**

# Water-Energy Nexus: A dynamic study of multi-pumps water station powered by grid-connected PV generator

This paper aims to investigate a full value energy chain using a grid-connected PV (GCPV) generator and a full value water chain meaning by three pumping units, the basic substructures of water-energy nexus. A dynamic study is exploited to elucidate the different operating modes that can be encountered and more enlighten the interdependence in water and energy by exploiting the sustainability in energy-providing to save water. In the side of the GCPV generator, Voltage Oriented Control (VOC) strategy is used to maintain the stability of the voltage DC bus and control the reactive power between the grid and the PV array. The water system is composed of three identical pumping units which make them useful whatever the irradiance. Here, Power-Field Oriented Control (P-FOC) is used in each pumping unit in order to control the absorbed power and the magnetic state of the induction motor coupled to the used centrifugal pump. On that account, by amending the intermittence of the solar irradiance and the needed water volume, the water-energy nexus concept is being more substantial and makes more practically the used system in rural areas and agriculture zones, which in turn represents the most belief ideology in the developed policies.

*Keywords: grid connected PV generator, water station, water-energy nexus, Voltage Oriented Control, Power-Field Oriented Control.*

*Article history: Received 23 December 2019, Accepted 17 May 2020*

## 1. Introduction

In order to achieve a sustainable development, the actual policies appear obligated to address the water and the clean electricity. Traditionally, these two concerns are treated separately. However, they are closely interdependent which termed by clean energy-water nexus which is defined as follow.

Clean energy-water nexus is a one architecture composed by two infrastructures, the first is devoted to describe a full energy value chain and the second describes a full water value chain [1-3].

In order to expand the utility of these architectures to high-level policy decision, the developed countries pick up their attentions to this concept in different vital sectors. Therefore, it's added to the integrated perspective prior in academic research. Previously, in agriculture, the researches carried out have explored only the energy or water or impact of specific technology used in order to minimize the electricity consumption or augmentation of water production [4, 5]. Coupling of these two fulfilments represent the basic idea of energy water nexus.

[*] Corresponding author: Université de Tunis, ENSIT, 1008 Montfleury, Tunisia, E-mail: mondher.a@yahoo.com
[1] Université de Tunis, ENSIT, 1008 Montfleury, Tunisia
[2] Université de Tunis El Manar, ENIT, LR11ES15 LSE BP 1002, Tunis, Tunisia
[3] Université de Tunis Carthage, ENSTAB, 1022 Hammam-Chott, Tunisia
Amine Ben Rhouma E-mail : amine.benrhouma@enit.rnu.tn
Jamel Belhadj E-mail : Jamel.Belhadj@ensit.rnu.tn

In this context, this paper proposes a model and a smart control strategy of a grid connected PV system feeding a water pumping station in order to coupling a full energy chain and a full water chain. The water station is composed by three pumps (1 HP) and exploit the power modularity technic to operate the maximum produced power with preference of pumping water. The control strategies used in the considered system are VOC in side of distribution network [6], and P-FOC for the three pumping units [7]. Generally, using these controllers allows, with the freedom degrees offered, the control of DC link voltage to extract the maximum produced power, and the reactive power exchange between the SPV array and the distribution network, by grid side, the magnetic state and the absorbed power of each induction motor by the side of water station.

The interdependence of water and clean energy in the proposed system, considering the intermittency and water volume needed, bring out four operating modes [8, 9]. These different modes clarify more and more the cooperation between the water station and the grid connected decentralized source. Furthermore, clean energy and water nexus provide invincible benefits : improve power yield and the overall system efficiency, additional to the cost reduction due to the elimination of storage system cost [10].

This paper is organized as follows: Section 2 is dedicated to expose the proposed system in order to more clarify the architecture and the different operating modes. Section 3 exposes the modelling. Afterwards, the simulation results are shown in the section 4. Finally, the conclusion, the appendix and the references are on view at the end of the paper.

## *2. Proposed system & operating modes*

This section is composed by two subsections. The first is devoted to explore the general architecture and analyze of the investigated control strategy of the considered system. The second is dedicated to inspect the different operating modes produced with consideration of constraints of the intermittency of the distributed generation and the water volume.

### 2.1. Architecture and overview of control strategies

The proposed system consists of water station powered by a grid connected PV generator. At standard test conditions, the solar PV generator is able to produce 5 kW. The DC link voltage is chosen to be 650 V. The water station is composed by three pumping units connected in parallel. Each unit is formed by an induction motor coupled with a VSC who deliver a mechanical power to the pump. Each pumping unit is connected to the same DC link mentioned above. The detailed specification and parameters of the motor are illustrated in Table I.

The architecture of the proposed system is showed by the Fig. 1. The uses of several pumps allow to improve the efficiency of the motor-pumps as described below.

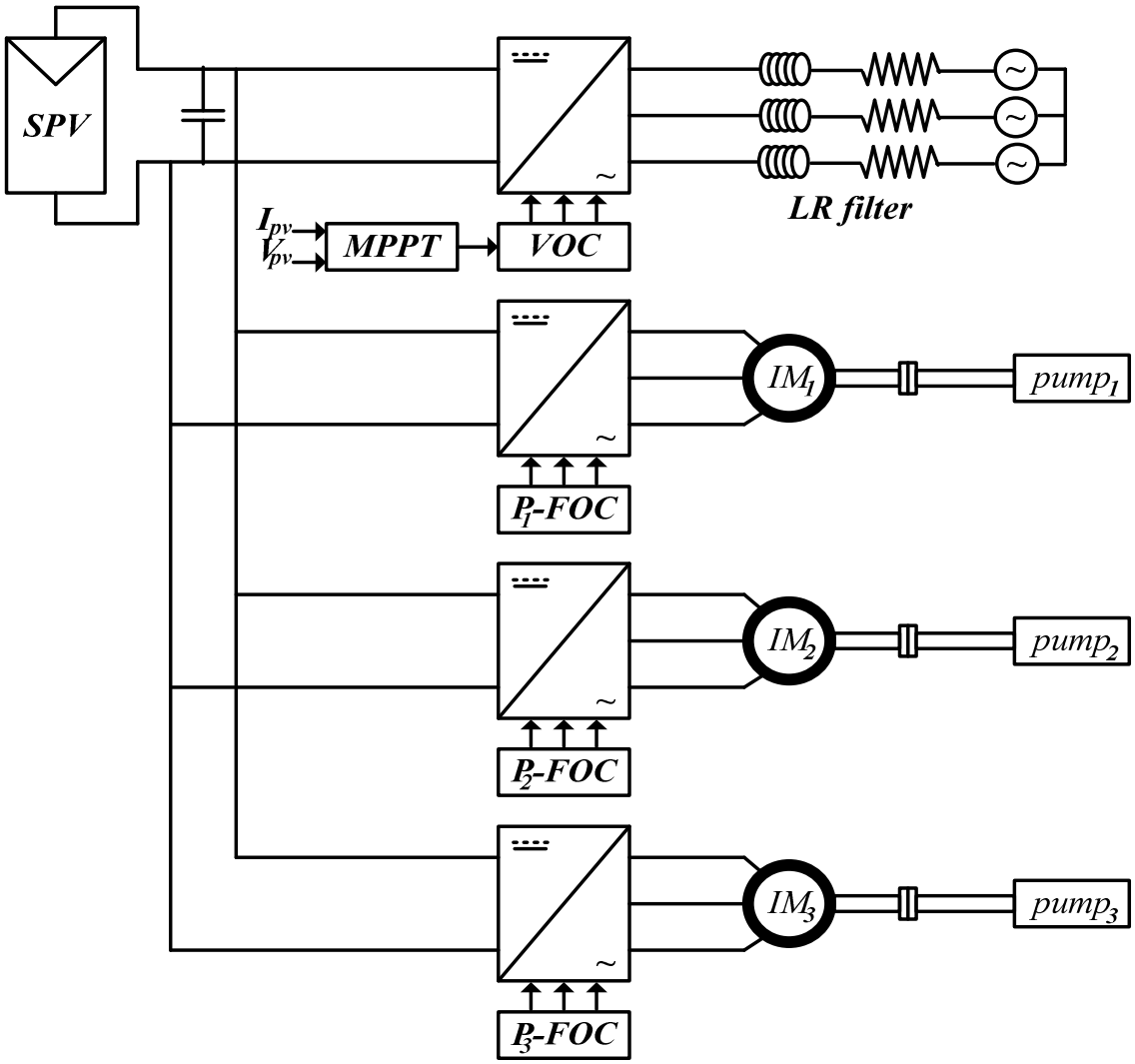


Fig. 1. System architecture

The first subsystem is devoted in general terms to describe the power source in the system. In fact, it's necessary to connect a Power Conditioning Unit (PCU) between the PV generator and the utility grid. In our case, a DC/AC inverter is used and must be able to fulfill two problems. The first is devoted to extract the maximal power point from the PV generator through an MPPT algorithm and the second is devoted to adapt the form of energy in the two side of the subsystem via a targeted control strategy.

The second subsystem is devoted to produce the water, it's composed of three identical pumping unit, each pumping unit is formed by an induction motor (IM) and a centrifugal pump. The IM specification and characteristics are given in Table I.

### 2.2. Operating modes

The needed water volume and variability of the produced power are considered as constraints to provide four functioning modes which are explained in this section.

A control strategy and a smart power sharing exploited in our architecture to shed light the cooperation of energy and water to reach a satisfactory water energy efficiency and

sustainable services.

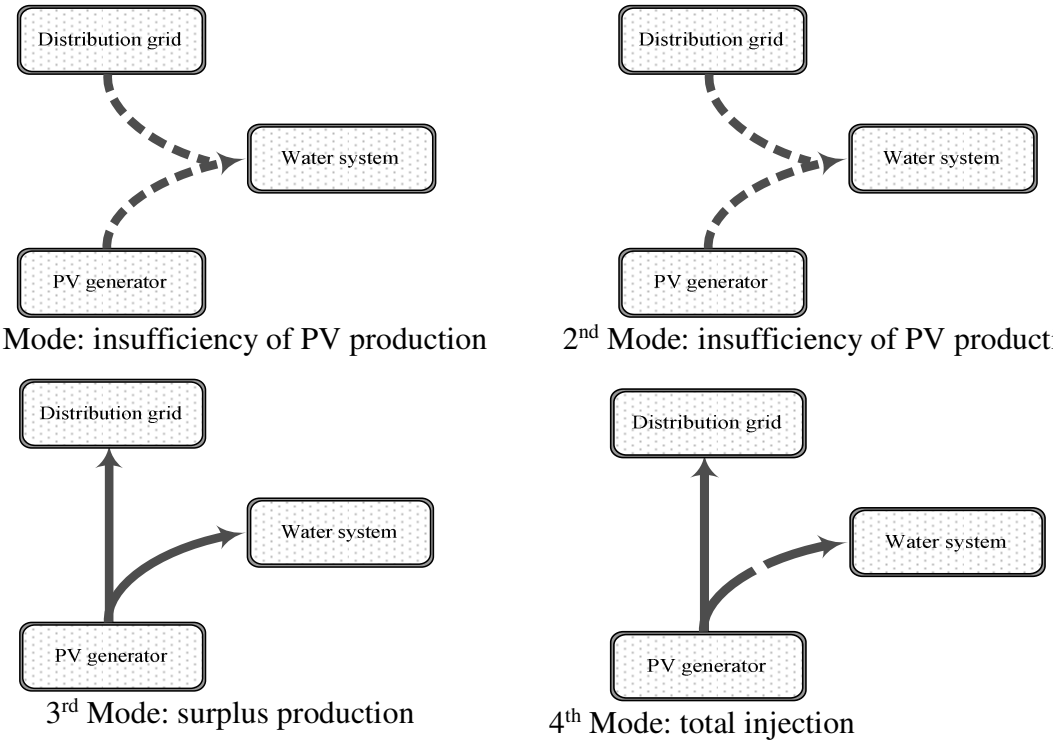


Fig. 2. Different operating modes

The exploitation of the freedom degrees aimed previously provides four operating modes. The first is when we need water, but there is no produced power through PV able to operate the water system. The distribution network supports the insufficiency. When the produced power is equal to demanded power, this mode is called photovoltaic pumping. As well as, the production is upper than the demanded power, which represent the third mode, the distribution network plays the role of storage system. Finally, when there are no needs of water, the produced energy is totally injected to the distribution network.

## *3. System modelling*

### 3.1. PV generator

The direct conversion of solar irradiation to an electrical energy is obtained by a photovoltaic cell. The non-ideal characteristic ( $I_{pv} - V_{pv}$ ) of solar module is given by Eq (1) [11-13].

$$I_c = I_{ph} - I_0 \cdot \left[ \exp\left( \frac{\left(V_c + R_s . I_c\right)}{N_s . V_t} \right) - 1 \right] - \frac{V_c + R_s . I_c}{R_{sh}} \qquad \textbf{(1)}$$

Where $I_{ph}$ is the photovoltaic current, $I_0$ is the saturation current, $N_s$ is cells connected in series and the thermal voltage $V_t = \dfrac{a.k.T}{q}$ where $a$ is the diode ideality

factor, $T$ is the cell temperature, $k$ is Boltzmann constant and $q$ is the electron charge. The above figure represents the equivalent circuit of the photovoltaic cell.

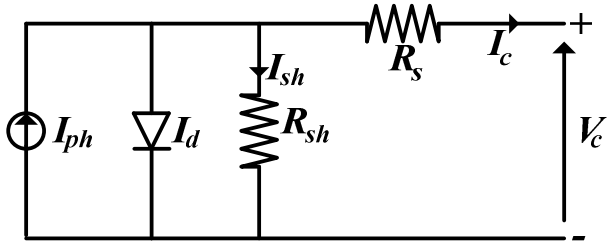


Fig. 3. Theoretical single diode photovoltaic module including shunt and series resistance

A module is a set of cells connected in series. An array is composed by several photovoltaic module connected in series in order to increase the voltage and in parallel in order to increase the current. The Eq (2) is the non-ideal model of the photovoltaic array.

$$I_{pv} = N_p.I_{ph} - N_p.I_0.\left[\exp\left(\frac{\left(V_c + R_s.I_c\right)}{N_s.V_t}\right) - 1\right] - N_p\frac{V_c + R_s.I_c}{R_{sh}} \quad \textbf{(2)}$$

### 3.2. Grid modelling

It's clear from Eq (2) that the PV generator can be replaced by a current source. Practically, in link with the capacitor, the current variation involved a variation of voltage in terminals. Fig. 4. represents the global electrical circuit described the behavior of a single stage grid connected PV generator exploited in our system.

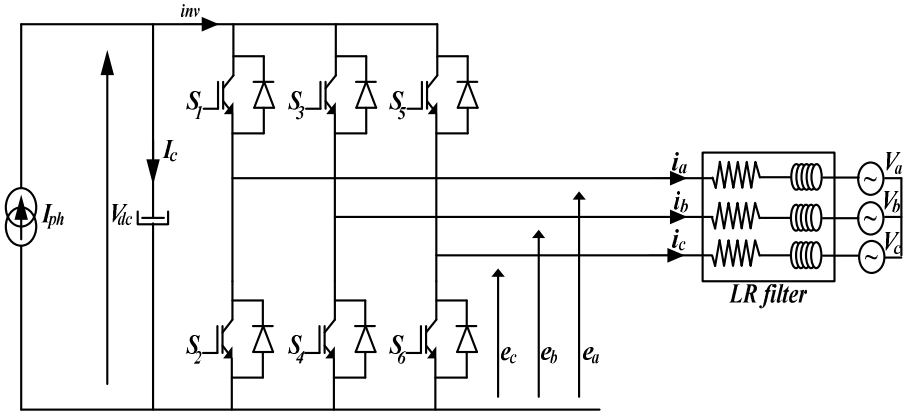


Fig. 4. Distribution network associated to VSI model

Basically, the mathematical model of electrical network is described by the following equations.

$$\begin{cases} V_a = V_m.\cos\left(2\pi ft\right) \\ V_b = V_m.\cos\left(2\pi ft - 2\pi/3\right) \\ V_c = V_m.\cos\left(2\pi ft - 4\pi/3\right) \end{cases} \quad \textbf{(3)}$$

Fig. 4. represents a VSI connected to the distribution grid through an RL filter. The mathematical model in a stationary frame $abc$ of inverter is given by the following equations [6].

$$\begin{cases} L\dfrac{di_a}{dt} = -V_a - R.i_a + \left( S_1 - \dfrac{S_1+S_2+S_3}{3} \right).V_{dc} \\ L\dfrac{di_b}{dt} = -V_b - R.i_b + \left( S_2 - \dfrac{S_1+S_2+S_3}{3} \right).V_{dc} \\ L\dfrac{di_c}{dt} = -V_c - R.i_c + \left( S_3 - \dfrac{S_1+S_2+S_3}{3} \right).V_{dc} \end{cases} \quad \textbf{(4)}$$

### 3.1. Pumping unit modelling

As mentioned above, the pumping system is composed by a centrifugal pump driven by an induction machine. The induction machine is coupled to the DC bus by means of an inverter. The mechanical produced power is transferred to a centrifugal pump. In our case, the pump model determines the dependence between hydraulic pressure $P_r$ and the flow rate $Q$. The used model is depicted in Eq (5) and Eq (6). These equations interpret the conversation of the mechanical and the hydraulic domain without considering the hydraulic losses. The term $\Omega$ represents the motor speed. In turn, this speed will be applied to the centrifugal pump wheel in order to transform it to hydraulic power.

$$C_r = a.\Omega.Q + b.Q^2 \quad \textbf{(5)}$$

$$P_r = a.\Omega^2 + b.\Omega.Q + c.Q^2 \quad \textbf{(6)}$$

Where $a, b$ and $c$ can be determined using the characteristic curve (flow-pressure) or experimentally, these parameters are exposed in Table II in the appendix.
The Eq (7) represent the hydraulic loads which depend on two parameters: the hydraulic losses in pipes and the static pressure $P_s$. From this equation, we can determine the flow rate [14].

$$\begin{aligned} P_r &= P_s + k.Q^2 \\ P_s &= \rho.g.H_s \\ Q &= \sqrt{\frac{P_r - \rho.g.H_s}{k}} \end{aligned} \quad \textbf{(7)}$$

Where $\rho$ is the water density, $g$ is the gravity, $H_s$ is the static height, $k$ the parameter due to the losses in the pipeline. Fig. 5. depicts the hydraulic network used in the simulation to provide the behavior of the pumping system.

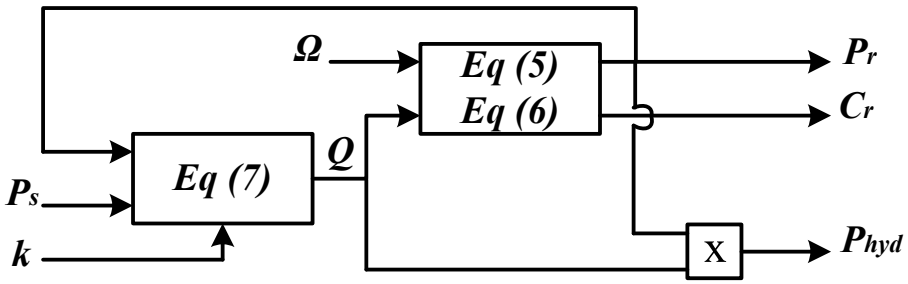


Fig. 5. Model of pumping unit

## 4. Simulation results and discussion

study was examined in order to validate the different control strategies firstly and evaluate the different operating modes, subsequently.

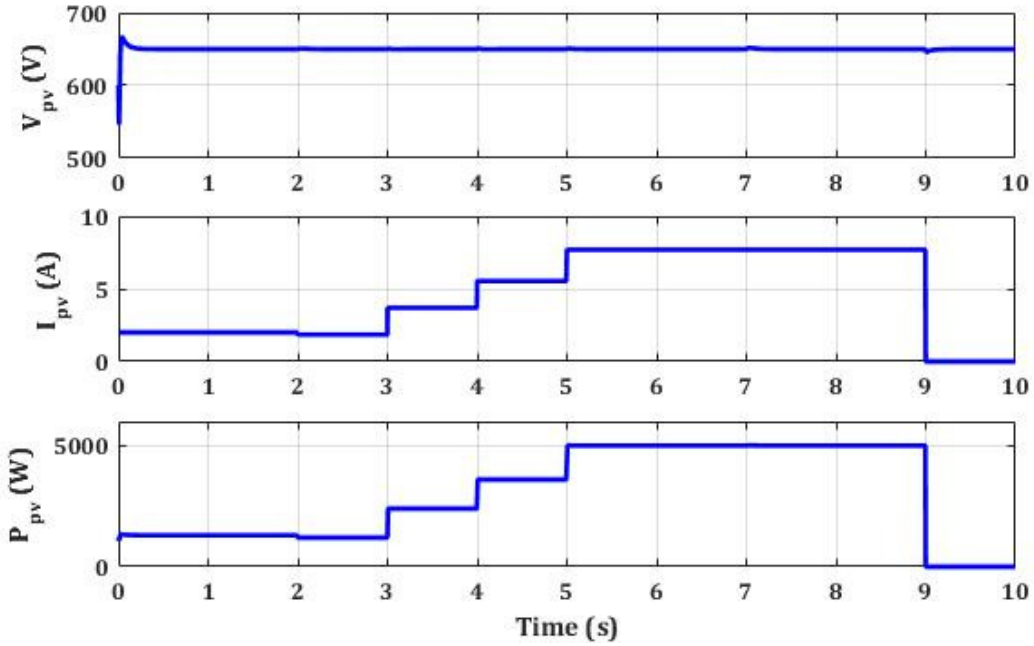


Fig. 6. Current, voltage and power in DC bus

Fig. 6. shows the output current,voltage and power of SPV array in different level of solar radiation respectively (0.26kW/m², 0.24kW/m², 0.48kW/m², 0.72kW/m², 1kW/m² and 0kW/m²). As mentioned in section 3 a direct current source is able to deliver the operational power corresponding to the same solar radiation reported above. The solar radiation profile is chosen to establish the different functioning modes which will be discussed minutely below.

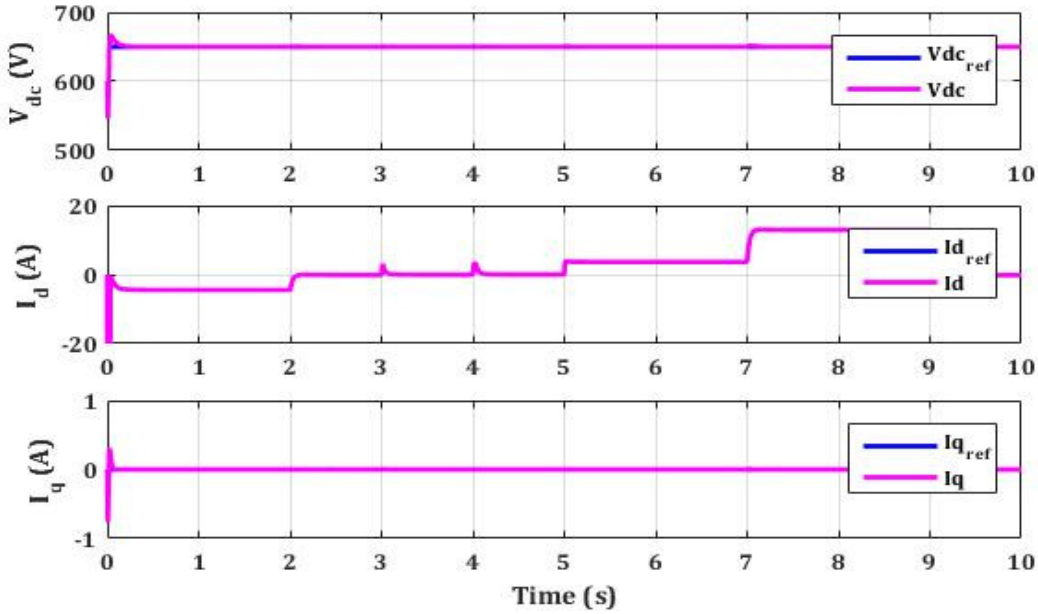


Fig. 7. (a). Grid connected PV system output response using VOC

Fig. 7. (a). illustrates the behavior of different control loops of the grid, the first show the voltage DC link loop. It can be seen that the voltage profile well follows the reference cited previously at 650V. In the second , the active current is negative because the produced power is not enough to operate the water station. We can be in this situation if there is no water in the tank. Therefore, the distribution network supports the insufficiency. Hence, the mode 1 is present. Between 2 s and 5 s, pumping PV mode ($2^{nd}$ mode) is executed, which explained the absence of active power injection. At 2 s, only the first pumping unit is operational, at 3 s, the second pumping unit started. These two second is considered as a partial functioning PV pumping mode. At 4 s, the third unit is functional, which means total functioning of the PV pumping. Subsequently, we are in case of the third mode during the two next seconds. The produces power is upper than the total consumed power. Consequently, the surplus power is delivered to the grid. For the next two second, between 7 s and 9 s, the needed volume of water is reached, therefore pumping water is not requested. So, the produced power is totally injected in the grid, meaning the settlement of the fourth mode. The last figure presents the reactive current evolution. It's set at zero during all over the simulation.

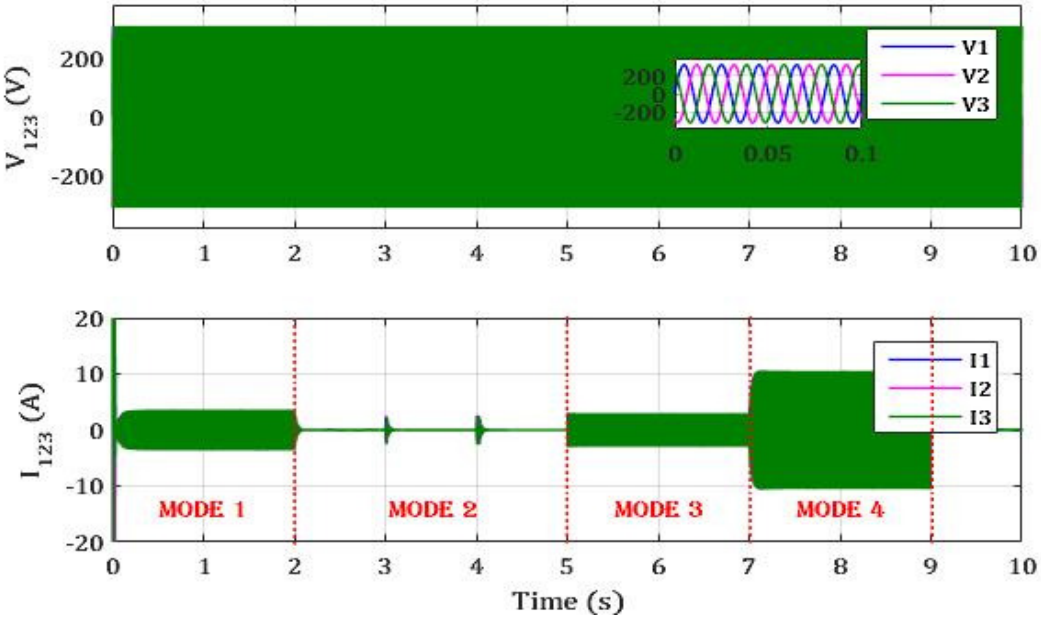


Fig. 7. (b). evolution of three phase voltage and current in grid in different operating modes

In Fig. 7. (b). the three-phase of voltage and current in the grid are exposed with distinction of the different operating modes.

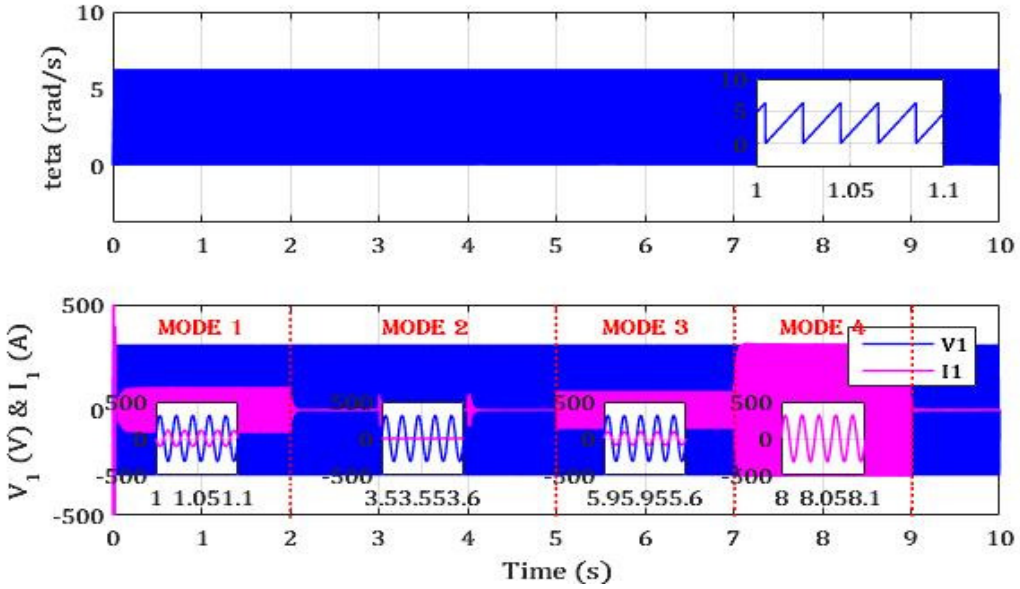


Fig. 7. (c). synchronization angle, first phase voltage and current in different operating modes

In Fig 7. (c), the detection algorithm show that the Phase Locked Loop allows a good performance in extraction of the grid phase. In addition, to more clarify the evolution of the different currents phases compared to the different voltage phases, the first phase current, multiplied by 30 to well appear it, and voltage are exposed. In the first mode, it's clear that the current and the voltage are in phase opposition, which explain the negativity of the direct current. In the second mode, as there is no injection, the current is set to zero. At the stage of injection, the current and the voltage are in phase as is apparent in the second figure.

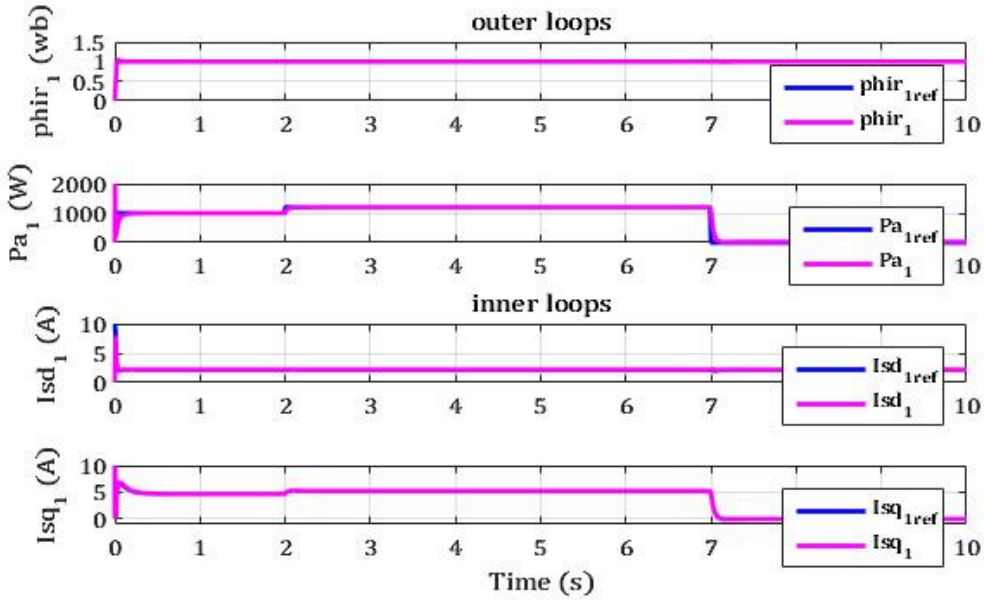


Fig. 8. (a). First induction machine performance using P-FOC

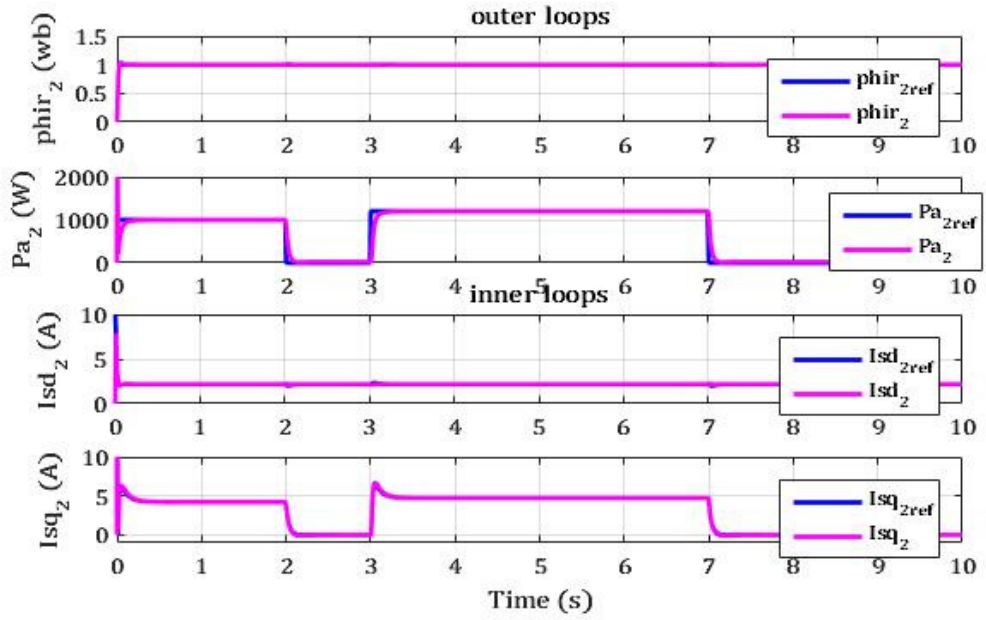


Fig. 8. (b). Second induction motor dynamic response using P-FOC

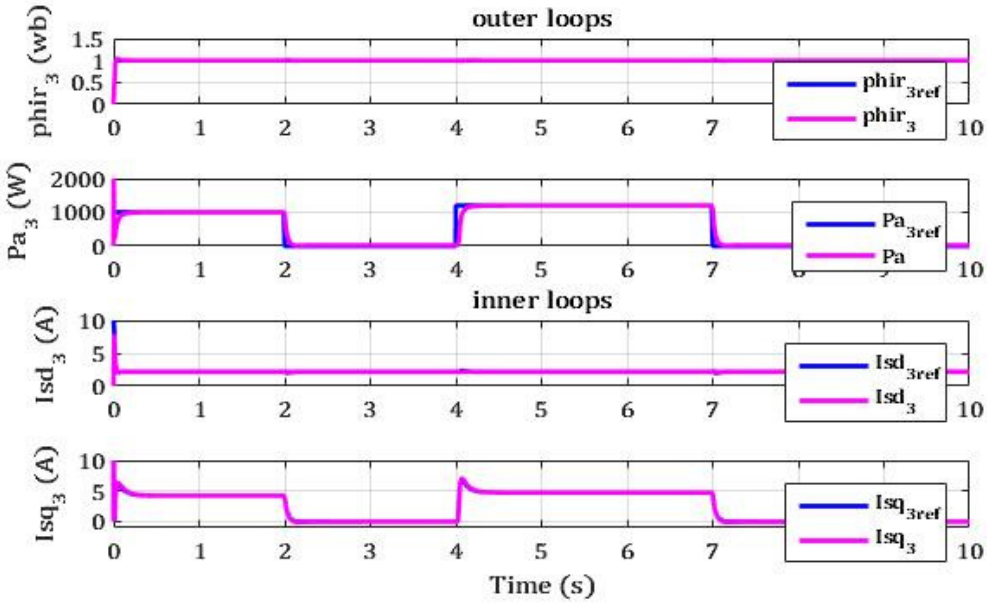


Fig. 8. (c). Third induction machine control output with P-FOC

Fig. 8.(a)-(b)-(c). show the performance of the different control loops of three induction motors used in the water station under a constant frequency 50 Hz. In the two first seconds, where there is needs of water and there is no produced power which able to make the water station operates in rated power, then, it shares 3kW. The grid rewards the gap which explain the first operating mode. After that, the first pumping unit is in functioning at the rated power, the second and the third units are not in function, because the minimal level of water in the tank is achieved, and the produced power is able to make functioning only the first unit. Then, at 3 s, the second unit is in functioning when the available power is able to make operates the two first pumping units. At 4 s, when the produced power is capable to put all over the water station operates, the last unit start sawing water. In this stage, as it's reported before, the PV pumping mode is present. After that, the available power in DC link is superior than the 3.6 kW, the power is adequate to make the whole station in work and the excessive power will be injected to the grid. Thus, we are in the phase of surplus production. Then, after 7 s, the total produced power is injected that explains the satisfaction in terms of requested water.

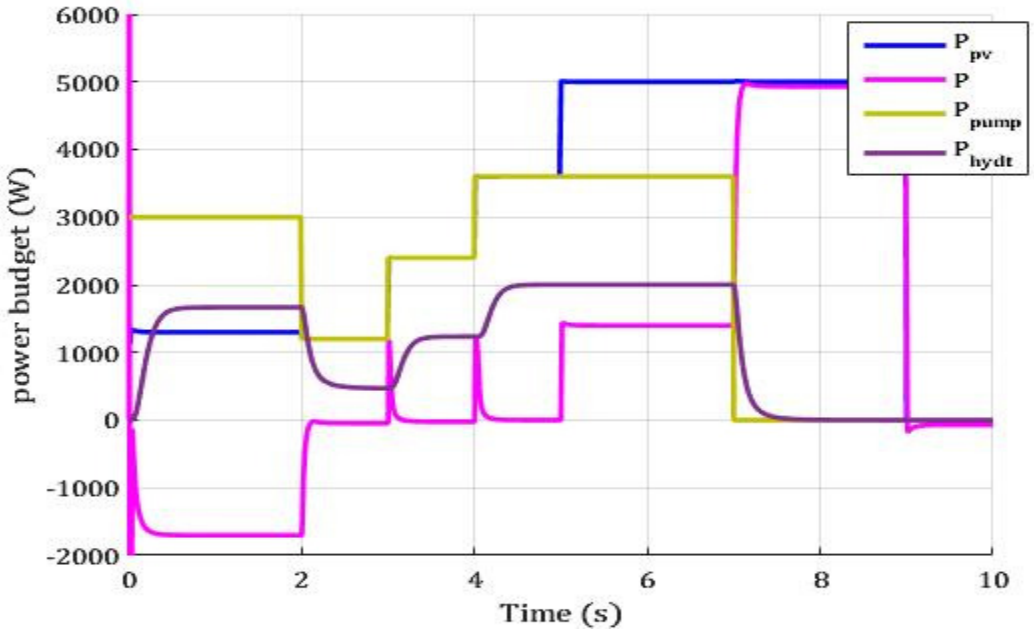


Fig. 9. Highlighted power

Fig. 9. Shows the differnts power existing in the system. Refering to this figure we can conclude :

$$P_{pump} = P_{pv} - P_{DN} \quad \textbf{(8)}$$

Where $P_{pump}$ is the power consumed by the water station, $P_{pv}$ is the produced power and $P_{DN}$ is the power distribution network. Note that also the hydraulic power is illustrated in the figure which is in terms of the pumping power, they are related by:

$$P_{hyd} = \eta . P_{pump} \quad \textbf{(9)}$$

Where $\eta$ is the yield of the pumping station. It represents the product of three pumping units. Each pumping unit yield is the product of the yield of the induction motor and its associated pump. The hydraulic power can be obtained also by multiplying the hydraulic parameters (flow and pressure) which represented in Fig. 10. (a)-(b).

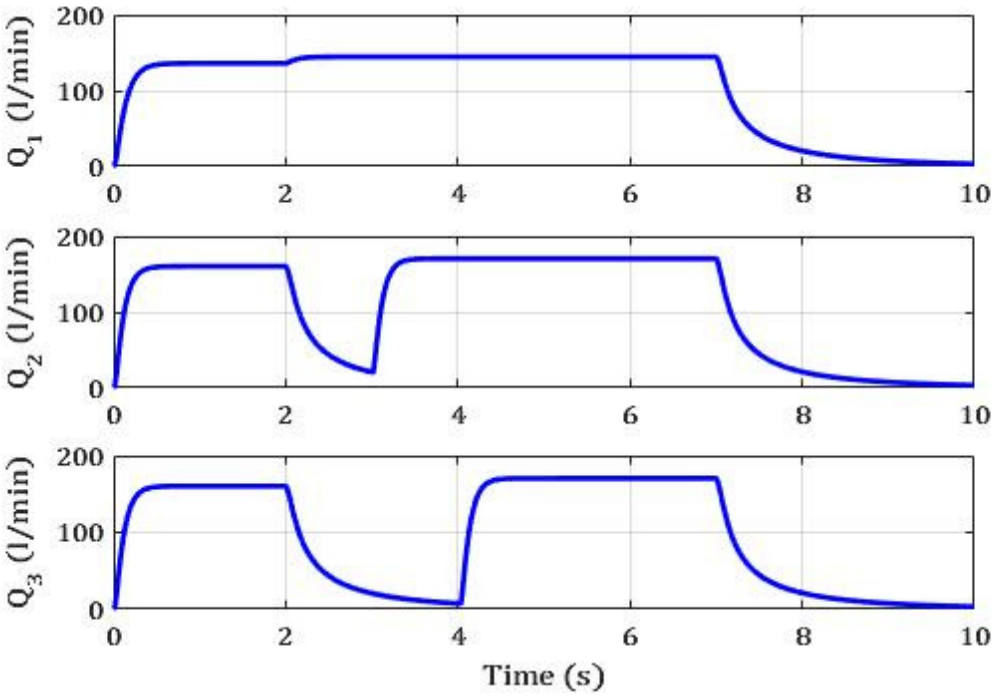


Fig. 10. (a). flow of water in three pumping system

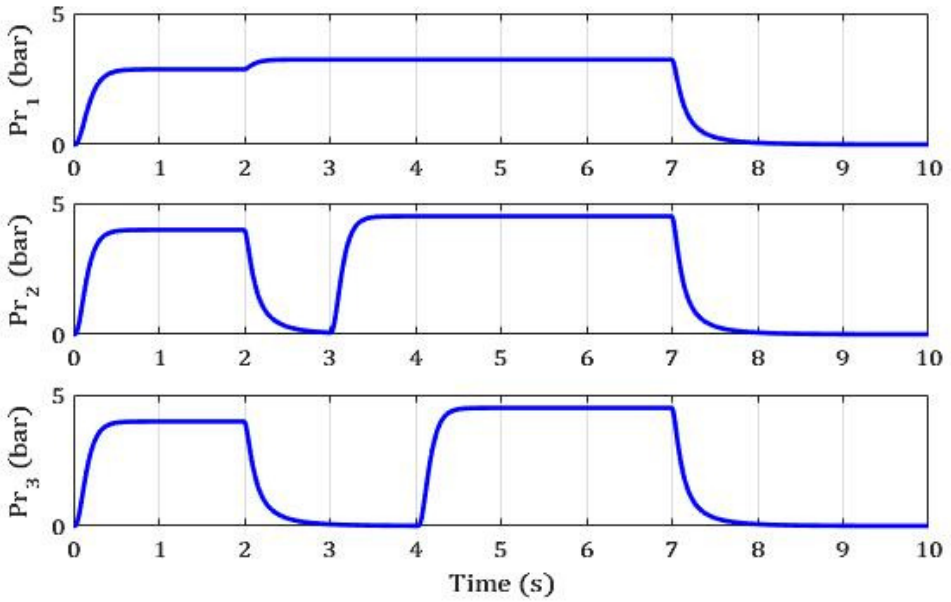


Fig. 10. (b). Pressure in three pumping system

It's clear from the two figure presented above that the hydraulic model used in the simulation is accurate. It follows exactly the different state of the induction motor with taking into account the consumed power. At the two first seconds, each pump absorb 1 kW, the flow and the pressure is not the same when the consumed power is 1.2 kW. The increase of the absorbed power results an increasing in flow and pressure.

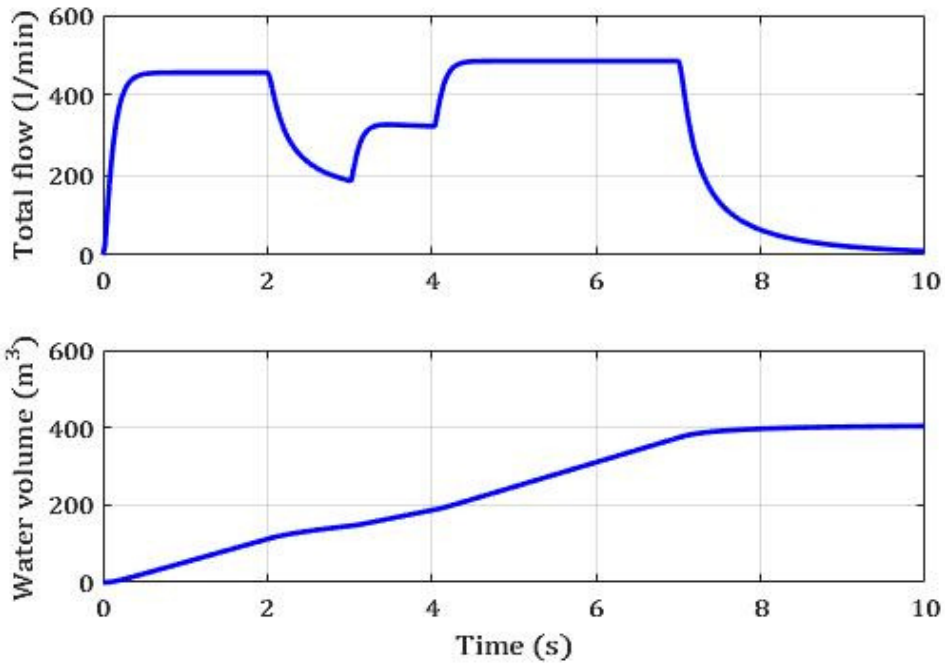


Fig. 11. Total flow and its corresponding pumped water volume

In Fig. 11. The total flow is shown in the first figure. From this parameter we can obtain the volume of water which can be obtained in one day by using this equation:

$$V_{water} = \frac{24 \times 3600}{sim\_time} \times \int_{0H}^{24H} \left(Q_1 + Q_2 + Q_3\right) dt \qquad \textbf{(10)}$$

Where $Q_{(1,2,3)}$ is respectively the flow of the first, the second and the third pumping unit

## 5. Conclusion

To elucidate the benefits of coupling energy and a water system, in this paper, a full value energy chain (GCPV generator) and a full value water chain (three pumping units) are exploited in the same architecture. A dynamic study shows the satisfactory performance of the different elements of the system. In fact, the exploitation of the sustainability of energy providing engenders sustainability of water production. Different operating modes bring out considering the intermittence of the solar PV array and the water volume in the side of the water station. Thence, the proposed system can be well suited for rural and especially for agricultural even in residential zones, which put forward the natural water-energy nexus and their interdependence in the modern world.

**Appendix**

TABLE I
Induction motor specifications & parameters

| Specifications | | parameters | |
|---|---|---|---|
| Rated power | 750W | $R_s$ | $7.5\Omega$ |
| Rated voltage | 400V | $R_r$ | $11\Omega$ |
| Rated current | 2.5A | $L_s$ | $0.484H$ |
| Rated frequency | 50Hz | $L_r$ | $0.484H$ |
| rated speed | 2820rpm | $M$ | $0.46H$ |
| number of pole pairs | 1 | $f$ | $0.002N.m.s.rad^{-1}$ |
| | | $j$ | $0.003kg.m^2$ |

TABLE II
Hydraulic network parameters

| Symbol | values |
|---|---|
| $a$ | 0.000032 |
| $b$ | 0.0000982 |
| $c$ | 0.0000852 |

**Acknowledgment**

This work is supported by the Tunisian Ministry of High Education and Research, it was carried out in the LR11ES15 LSE, under ERANETMED NEXUS collaborative project "Energy and Water Systems Integration and Management", ID number 14-044 for the financial support.

## References


[1] A. M. Hamiche, A. B. Stambouli, and S. Flazi, "A review of the water-energy nexus," *Renewable and Sustainable Energy Reviews,* vol. 65, pp. 319-331, 2016.

[2] W. N. Lubega, and A. M. Farid, "Quantitative engineering systems modeling and analysis of the energy–water nexus," *Applied Energy,* vol. 135, pp. 142-157, 2014.

[3] W. N. Lubega, and A. M. Farid, "A reference system architecture for the energy–water nexus," *IEEE Systems Journal,* vol. 10, no. 1, pp. 106-116, 2014.

[4] E. Spang, W. Moomaw, K. Gallagher, P. Kirshen, and D. Marks, "The water consumption of energy production: an international comparison," *Environmental Research Letters,* vol. 9, no. 10, pp. 105002, 2014.

[5] C. J. Vörösmarty, P. B. McIntyre, M. O. Gessner, D. Dudgeon, A. Prusevich, P. Green, S. Glidden, S. E. Bunn, C. A. Sullivan, and C. R. Liermann, "Global threats to human water security and river biodiversity," *Nature,* vol. 467, no. 7315, pp. 555, 2010.

[6] R. Kadri, J.-P. Gaubert, and G. Champenois, "An improved maximum power point tracking for photovoltaic grid-connected inverter based on voltage-oriented control," *IEEE transactions on industrial electronics,* vol. 58, no. 1, pp. 66-75, 2010.

[7] A. B. Rhouma, J. Belhadj, and X. Roboam, "Control and energy management of a pumping system fed by hybrid Photovoltaic-Wind sources with hydraulic storage:-Static and dynamic analysis-"U/f" and "FOC" controls methods comparisons," *Journal of Electrical Systems,* vol. 4, no. 4, pp. 1-16, 2008.

[8] A. El Fadili, F. Cuny, A. El Magri, M. Stitou, F. Giri, J. Janik, and F. Chaoui, "Backstepping Control of Photovoltaic-Grid Hybrid Power Feed Water Pump," *IFAC-PapersOnLine,* vol. 50, no. 1, pp. 6540-6545, 2017.

[9] U. Sharma, and B. Singh, "Grid interactive bidirectional solar PV array fed water pumping system." pp. 1-6.

[10] R. Rawat, S. Kaushik, and R. Lamba, "A review on modeling, design methodology and size optimization of photovoltaic based water pumping, standalone and grid connected system," *Renewable and Sustainable Energy Reviews,* vol. 57, pp. 1506-1519, 2016.

[11] M. G. Villalva, J. R. Gazoli, and E. Ruppert Filho, "Modeling and circuit-based simulation of photovoltaic arrays." pp. 1244-1254.

[12] J. Loukil, and N. Derbel, "Control Strategy For a Photovoltaic/Lead-Acid Batteries Energy Production System," *Journal of Electrical Systems,* vol. 15, no. 3, pp. 459-479, 2019.

[13] S. Guesmi, M. Ghariani, M. Ayadi, and R. Neji, "Complete modeling of photovoltaic module with electrical parameters," *J. Automation & Systems Engineering,* vol. 11, no. 2, pp. 163-172, 2017.

[14] A. B. Rhouma, J. Belhadj, and X. Roboam, "Experimental characterization and energy analysis for water pumping system fed by intermittent source." pp. 1-6.